Site and bond percolation thresholds on regular lattices with compact extended-range neighborhoods in two and three dimensions

Zhipeng Xun [*] and Dapeng Hao [†]
School of Material Sciences and Physics, China University of Mining and Technology, Xuzhou 221116, China

Robert M. Ziff [‡]
Center for the Study of Complex System and Department of Chemical Engineering, University of Michigan, Ann Arbor, Michigan 48109-2800, USA

(Received 30 November 2021; accepted 13 January 2022; published 3 February 2022)

Extended-range percolation on various regular lattices, including all 11 Archimedean lattices in two dimensions and the simple cubic (SC), body-centered cubic (BCC), and face-centered cubic (FCC) lattices in three dimensions, is investigated. In two dimensions, correlations between coordination number z and site thresholds p_c for Archimedean lattices up to 10th nearest neighbors (NN) are seen by plotting z versus $1/p_c$ and z versus $-1/\ln(1-p_c)$ using the data of d'Iribarne *et al.* [J. Phys. A **32**, 2611 (1999)] and others. The results show that all the plots overlap on a line with a slope consistent with the theoretically predicted asymptotic value of $zp_c \sim 4\eta_c = 4.51235$, where η_c is the continuum threshold for disks. In three dimensions, precise site and bond thresholds for BCC and FCC lattices with 2nd and 3rd NN, and bond thresholds for the SC lattice with up to the 13th NN, are obtained by Monte Carlo simulations, using an efficient single-cluster growth method. For site percolation, the values of thresholds for different types of lattices with compact neighborhoods also collapse together, and linear fitting is consistent with the predicted value of $zp_c \sim 8\eta_c = 2.7351$, where η_c is the continuum threshold for spheres. For bond percolation, Bethe-lattice behavior $p_c = 1/(z-1)$ is expected to hold for large z, and the finite-z correction is confirmed to satisfy $zp_c - 1 \sim a_1 z^{-x}$, with $x = 2/3$ for three dimensions as predicted by Frei and Perkins [Electron. J. Probab. **21**, 56 (2016)] and by Xu *et al.* [Phys. Rev. E **103**, 022127 (2021)]. Our analysis indicates that for compact neighborhoods, the asymptotic behavior of zp_c has universal properties, depending only on the dimension of the system and whether site or bond percolation but not on the type of lattice.

DOI: 10.1103/PhysRevE.105.024105

I. INTRODUCTION

It is well known that percolation is an important model in statistical physics [1,2]. As a paradigmatic model, it can describe diverse phenomena in various fields, such as liquids moving in porous media [3,4], forest-fire problems [5,6], and epidemics [7,8]. Considering percolation on a lattice, each edge (vertex) is occupied by a bond (site) with probability p, and clusters of neighboring occupied sites or connected bonds can be constructed. As p increases, the clusters become larger, and at the threshold point p_c, an infinite cluster spanning over the whole lattice emerges. Over the past several decades, a tremendous amount of work has gone into finding exact or approximate values of the percolation thresholds for a variety of systems, as well as finding formulas to approximately predict those thresholds.

Many kinds of percolation models have been established. The most common one is to occupy sites or bonds on a regular lattice with statistically independent probability p. Site and bond percolation can be distinguished depending on the method of obtaining the cluster. One can also consider continuum percolation systems [9–12], such as overlapping disks and spheres placed randomly. Further variations involve correlated percolation [13,14], like for example drilling percolation [15,16]. In bootstrap percolation [17–20], sites and/or bonds are first occupied and then successively culled from a system if a site does not have at least k neighbors. Another important model of percolation, which is in a different universality class, is directed percolation [21–24], where connectivity along a bond depends on the direction of the flow.

Among numerous models, percolation on lattices with extended neighborhoods has been of longstanding interest. In fact, this kind of percolation system has many applications. For example, site percolation on lattices with extended neighborhoods relates to problems of adsorption of extended shapes on a lattice, such as disks and squares [25,26], and bond percolation with extended neighbors has long-range links similar to small-world networks [27]. In addition, bond percolation with extended neighbors is also similar to spatial models of the spread of epidemics via long-range links [28]. Just recently [8], it was pointed out how the threshold is related to the basic epidemic infectivity parameter R_0, for trees (Bethe lattice), trees with triangular cliques, and nonplanar lattices with extended-range connectivity.

[*] zpxun@cumt.edu.cn
[†] dphao@cumt.edu.cn
[‡] rziff@umich.edu

The investigation of percolation on lattices with extended neighborhoods dates back to the "equivalent neighbor model" of Dalton, Domb, and Sykes from 1964 [29–31], and numerous studies have appeared since then. Extended-range site percolation on compact regions in a diamond shape on a square lattice, up to lattice distance of 10, was studied by Gouker and Family [32]. Other lattices, including body-centered cubic (BCC) and face-centered cubic (FCC) with extended neighborhoods, have also been studied [33,34]. d'Iribarne, Rasigni, and Rasigni [35–37] studied site percolation on all 11 Archimedean lattices ("mosaics") with extended-range connections up to the 10th nearest neighbors (NN), which we will discuss in detail later. It has been suggested that these results may be applicable to a model of constrained percolation [38]. Malarz and coworkers [39–46] carried out extensive numerical simulations on lattices with combinations of "complex neighborhoods" in two, three, and four dimensions. Koza and collaborators [25,26] studied percolation of overlapping shapes on a lattice, which can be mapped to extended-range site percolation. While much of the earlier work concerned site percolation, bond percolation on extended lattices has been studied more extensively recently [9,47–50].

Many studies have focused on exploring the correlations between percolation thresholds p_c and coordination number z or other properties of lattices. It has been argued [25,26,31,37] that for extended-range site percolation, the threshold p_c for large z can be related to the continuum percolation threshold η_c for objects of the same shape as the neighborhood, and this relationship is further clarified [51] by $p_c \sim 2^d \eta_c/z$, where d is the dimension of the system. In this paper, we show that the asymptotic behavior of zp_c for site percolation,

$$zp_c \sim 2^d \eta_c, \tag{1}$$

is indeed universal for neighborhoods limiting to a circle or sphere for z large. In the first task of this paper, we investigate site percolation of the 11 two-dimensional Archimedean lattices and the three-dimensional simple cubic (SC), BCC, and FCC lattices with extended neighbor connections. By fitting the data to the forms z versus $1/p_c$ and z versus $-1/\ln(1-p_c)$, we find good agreement with the predicted behavior of Eq. (1) with $4\eta_c = 4.51235$ for lattices in two dimensions and $8\eta_c = 2.7351$ for lattices in three dimensions, suggesting a universal asymptotic behavior of zp_c for lattices with compact extended neighborhoods.

For bond percolation, one expects that Bethe-lattice behavior $p_c = 1/(z-1)$ to hold for large z, because for large z and small p, the chance of hitting the same site twice is low and the system behaves basically like a tree [52]. Theoretical analysis of finite-z corrections for bond thresholds has recently been given by Frei and Perkins [53], Hong [54], and Xu *et al.* [9] as

$$zp_c - 1 \sim a_1 z^{-x}, \tag{2}$$

where $x = (d-1)/d$ for $d = 2, 3$, implying $x = 1/2$ in two dimensions and $2/3$ in three dimensions. In the second task of this paper, we study bond percolation on three-dimensional SC, BCC, and FCC lattices with extended neighborhoods by Monte Carlo simulation using a single-cluster growth algorithm. We find many precise bond percolation thresholds, and data fitting is consistent with Eq. (2) with $x = 2/3$.

The remainder of the paper is organized as follows. Section II describes the theoretical prediction of the asymptotic behavior of zp_c for site percolation. The results and analysis in two and three dimensions are given in Sec. III and Sec. IV, respectively, and in Sec. V we present our conclusions.

II. THEORETICAL ANALYSIS

We analyze the effective extended-range neighborhood for an object of an arbitrary shape. First we consider a continuum system of volume V with the random placement of N overlapping objects of the given shape. The continuum percolation threshold η_c represents the total volume fraction of the adsorbed objects, including overlapping volume, at the critical point

$$\eta_c = a_d r^d \frac{N}{V}, \tag{3}$$

where r is the radius or other length scale of the object and $a_d r^d$ is its volume, with a_d depending on the shape of the object. Covering the space occupied by the objects with a fine mesh of any lattice type, the system can be mapped to site percolation on that lattice with an extended neighborhood of essentially the same shape but with a length scale $2r$ about the central point. The ratio $Nv_0/V = p_c$ corresponds to the site occupation threshold on the lattice, where v_0 is the area or volume per site. The effective z is equal to the number of sites within that region of influence of length scale $2r$,

$$z = a_d (2r)^d / v_0. \tag{4}$$

For example, for squares or cubes of length $2k$ on a square or cubic lattice with $v_0 = 1$ [55], $z = (2k)^d$. Then it follows from Eqs. (3) and (4) that

$$zp_c = [a_d (2r)^d / v_0](Nv_0/V) = 2^d (a_d r^d N/V) = 2^d \eta_c, \tag{5}$$

as given in Eq. (1). This equation should describe the behavior of p_c for large z where the objects become similar to a continuum, for systems with compact neighborhoods, and where η_c is the critical coverage for continuum systems of the shape of the neighborhood.

Figure 1 illustrates the situation where we have the continuum percolation of disks, here of radius 3, embedded on a kagome lattice of unit edge length. The system is seen to be equivalent to an extended-range percolation model with the centers of the disks being sites connected if they fall within a radius 6 with each other. The disk of radius 3 covers 27 sites on the lattice, while the range of the equivalent site percolation model covers 97 sites and extends to the 15th NN. Note here the number of sites in circle of radius 6 (97 sites) is not four times the number as in the disk (27 sites), as that ratio would be for larger circles or indeed objects of any shape according to Eq. (4).

We will choose neighborhoods with sites that fall within a radius r. As $z \to \infty$, the shape of the neighborhood becomes more circular (or spherical), so one can naturally suppose that the asymptotic behavior of zp_c should be universal, with η_c for a disk or spheres depending on the dimension of the system. For circular neighborhoods in two dimensions, where η_c for disks equals 1.128087 [9–12,56], one should thus expect

$$zp_c \sim 4.51235, \tag{6}$$

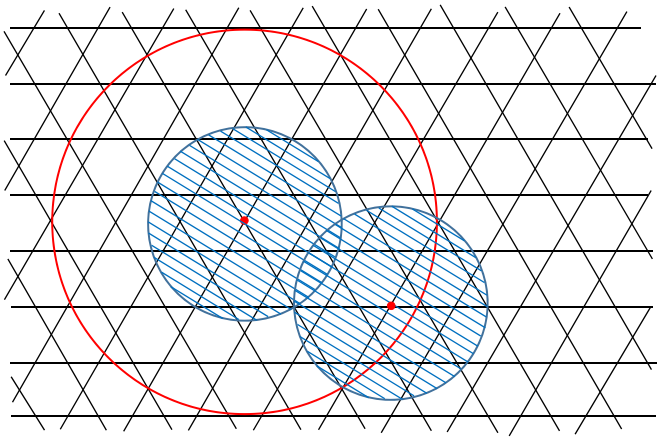

FIG. 1. Illustration showing the relation between continuum percolation of disks of radius 3, and the equivalent extended-range site percolation model of range 6, embedded on a kagome lattice. The smaller disk covers 27 sites while the larger one covers 97 sites and is equivalent to having $z = 96$ (we do not count the central site when considering z) with a range up to the 15th NN.

for large z, while for spherical neighborhoods in three dimensions, where η_c for spheres equals 0.34189 [57–59], one should expect

$$zp_c \sim 2.7351. \tag{7}$$

A related approach comes from Ref. [25], where Koza *et al.* investigated squares of size $k \times k$ and cubes of size $k \times k \times k$, randomly distributed in an overlapping manner on square or cubic lattices. The critical number (per site) of these objects for percolation between neighboring occupied sites defines the threshold p_c. At the percolation point, the fraction of sites on the lattice covered by at least one square or cube, $\phi_c(k)$, can be related to p_c by $\phi_c(k) = 1 - (1 - p_c)^{k^d}$, which can also be written as

$$p_c = 1 - [1 - \phi_c(k)]^{1/k^d}. \tag{8}$$

For large k, the model limits to the percolation of aligned squares or cubes on a continuum, and $\phi_c(k)$ limits to ϕ_c for the corresponding continuum system. Replacing $\phi_c(k)$ by the continuum value ϕ_c in Eq. (8), one obtains an approximation to find p_c for discrete hypercubic objects of volume k^d with large but finite k [25,26],

$$p_c = 1 - (1 - \phi_c)^{1/k^d}. \tag{9}$$

One defines η_c as the total area or volume of the objects placed or adsorbed in the system, including the area or volume of the overlapped parts, divided by the area or volume of the system. The quantity η_c is related to ϕ_c by $\phi_c = 1 - e^{-\eta_c}$ which can be substituted into Eq. (9) to yield

$$p_c = 1 - e^{-\eta_c/k^d}. \tag{10}$$

We can generalize Eq. (10) to objects of arbitrary shape and an arbitrary lattice by replacing k^d by $z/(2^d)$ (the number of sites in the neighborhood), yielding the general formula

$$p_c = 1 - e^{-2^d\eta_c/z}. \tag{11}$$

The above formula does not depend on the type of lattice (square, triangular, etc.) used, because for lattices with z NN, the number of sites of the equivalent object (disk, sphere, etc.) is always $z/(2^d)$. The type of lattice does not matter because the volume per lattice site v_0 cancels out, as seen in Eq. (5). Note that Eq. (11) was also given in Ref. [51], although without a complete derivation as given here.

Solving for z, Eq. (11) yields

$$z = \frac{2^d\eta_c}{-\ln(1 - p_c)}. \tag{12}$$

In the limit of large z, Eq. (11) limits to Eq. (1) and this gives an alternative derivation of that result. However, for moderate z, it has been found [51] that for some systems, Eq. (11) gives a better estimate of p_c than Eq. (1). One of the goals of this paper is to compare Eqs. (11) and (1) in modeling the finite-z behavior.

In Ref. [51], we also found that the finite-z effect can be taken into account by assuming $p_c = c/(z + b)$, where b and $c = 2^d\eta_c$ are constants. We can write this relation as

$$z = \frac{c}{p_c} - b. \tag{13}$$

In contrast to Eq. (12), this formula contains a new adjustable parameter, b. For more details about these formulas, one can also see Refs. [25,26,51].

Equations (12) and (13) show that if we plot z versus $-1/\ln(1 - p_c)$ or z versus $1/p_c$, one can directly get the value of $c = 2^d\eta_c$ from the slopes, and in the latter case, the value of $-b$ from the intercept.

III. SITE PERCOLATION ON ARCHIMEDEAN LATTICES WITH EXTENDED CONNECTIONS

Figure 2 shows drawings of the 11 Archimedean lattices, in which all polygons are regular and each vertex is surrounded by the same sequence of polygons. Each lattice is characterized by a standard notation; for example, the notation $(3^4, 6)$ means that each vertex is surrounded by four triangles and one hexagon, in that order.

In the late 1990s, d'Iribarne, Rasigni, and Rasigni [35–37] determined the site percolation thresholds of all Archimedean lattices with extended ranges up to the 10th NN. We have listed those thresholds in Table I, updated with more precise results in some cases [46,51], and precise thresholds for the standard lattices (with first NN). Furthermore, we can make use of the fact that some of the extended-range lattices are matching lattices of the same lattice with first NN and therefore have the complementary threshold $1 - p_c$, as shown in Fig. 3. (In a matching lattice, all faces with more than three sides are replaced by a complete graph that connects all pairs of vertices together.)

We can also find additional results by using the fact that a bond problem can be converted to a site problem by replacing the lattice by the line graph or covering lattice, which connects the centers of the bonds together to create a new lattice. The $(4, 8^2)$ lattice with first and second NN is the covering lattice of the square lattice with double bonds (the Lieb lattice),

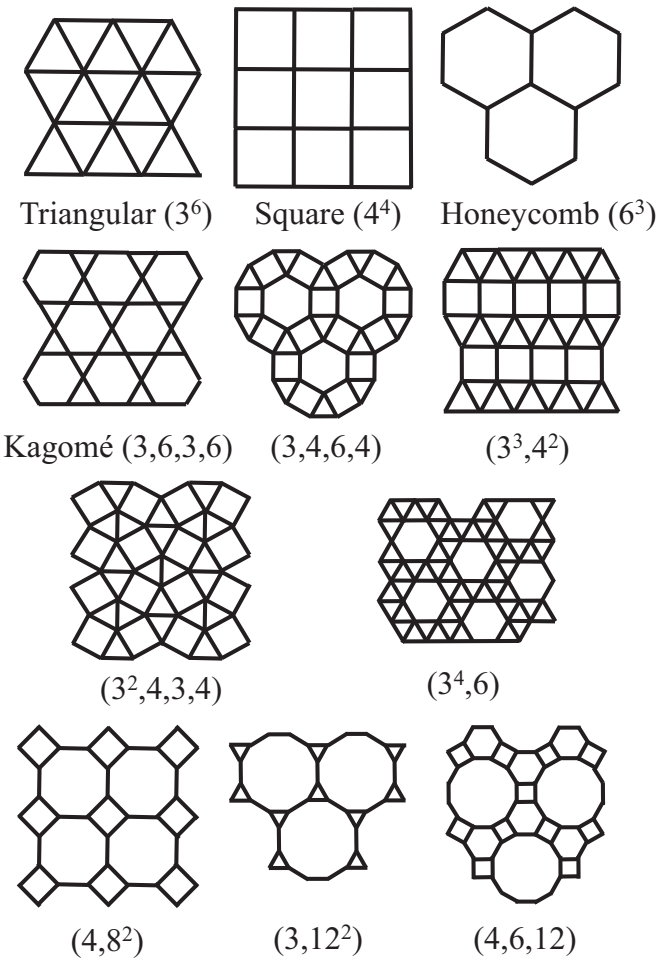

FIG. 2. Illustrations of the 11 Archimedean lattices.

with each bond having a threshold of $p_c = \sqrt{1/2}$, and consequently this is the site threshold of the $(4, 8^2)$ lattice with first and second NN bonds as shown in Fig. 4. The covering lattice of the kagome (3,6,3,6) lattice is the (3,4,6,4) lattice with first and second NN, and therefore the bond threshold of the kagome lattice 0.524405 is the site threshold of the (3,4,6,4)-1,2 lattice [Fig. 5(b)]. A similar construction on the kagome lattice with double bonds shows that the site threshold of the (4,6,12) lattice with first and second NN is equal to the square root of the bond threshold of the kagome lattice, $(0.524405)^{1/2} = 0.724158$ [Fig. 5(d)]. These results are all included in Table I. Comparing these improved values to

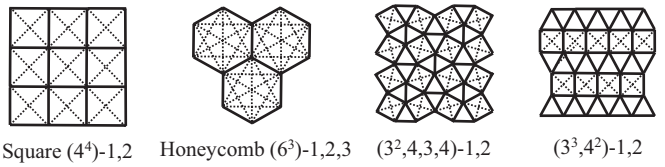

FIG. 3. Illustration showing that the matching lattices of these four Archimedean lattices are the same lattices with the first NN, the second NN, and in the honeycomb case, the third NN. The thresholds of these lattices is one minus the threshold of the same lattices with just the first NN.

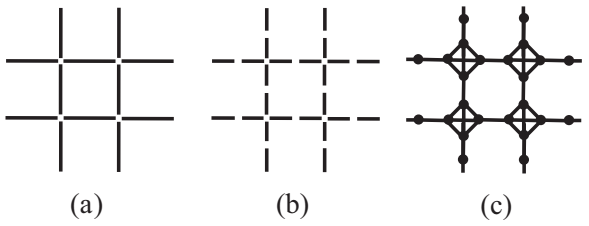

FIG. 4. Derivation of the threshold of the $(4, 8^2)$ lattice with first- and second-NN bonds by the bond-to-site (covering) transformation: (a) Bond percolation on a square lattice, p_c(bond) $= 1/2$. (b) Bond percolation on the square lattice with double bonds (the Lieb lattice), p_c(bond)$= 1/\sqrt{2}$. (c) Site percolation on the $(4, 8^2)$-1,2 lattice, p_c(site)$= 1/\sqrt{2}$.

those found by d'Iribarne *et al.*, we find that the latter are accurate to at least two digits, with some variation in the third digit; for example for the (4,6,12)-1,2 lattice, they give 0.720 compared to the value 0.724158 that we find above. Still, the results of d'Iribarne *et al.* are sufficiently accurate for our discussion of the general behavior of the thresholds. In Table I, we also list NN, the number of nearest neighbors in each shell, the total z up to that shell z_{total}, and the square of the radius of that shell r^2. An example of the first five shells of neighbors of the kagome (3,6,3,6) lattice is shown in Fig. 6.

Using the data of Table I, we plot the behavior of z versus $1/p_c$ and z versus $-1/\ln(1 - p_c)$, proposed by Eqs. (13) and (12), for the different lattices, in Figs. 7 and 8, respectively. In these plots, the discrete points represent the data for each lattice, and the virtual straight line is a guideline with a slope of 4.512 and intercept of zero representing Eq. (6). It is seen that nearly all the lattices collapse to the same line, and most of the plots give a slope near the predicted value of 4.512. The range of the fitted slope in Fig. 7 of the individual Archimedean lattices is 4.38 to 4.59, with errors from 0.02 to 0.09. The slopes of the individual curves in Fig. 8 vary from 4.30 to 4.56, with similar errors. The intercepts are -2.13 to -3.44 in Fig. 7 and 0.49 to $= -0.88$ for Fig. 8. Slopes and intercepts with errors for each lattice are listed in the Supplemental Material [62]. This result demonstrates the

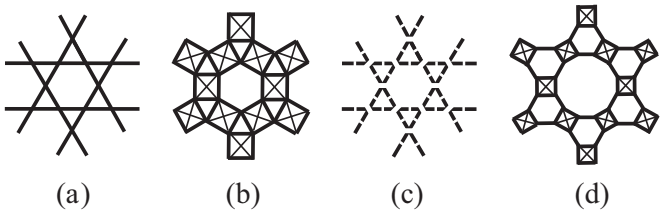

FIG. 5. (a) Kagome lattice with p_c(bond) $= 0.524405$ [60]. (b) Covering lattice of (a), the (3,4,6,4) lattice with first and second NN, with p_c(site) $= 0.524405$. (c) Kagome double-bond lattice with p_c(bond)$= (0.524405)^{1/2} = 0.724128$. (d) Covering lattice of (c), the (4,6,12) lattice with first and second NN, with p_c(site)$=$ 0.724128. Note you can go directly from (d) to (b) by replacing two sites along the inner edges of the hexagons by one site, so that the threshold p_c becomes squared, similar to the case of the $(3, 12^2)$ versus the (6^3) lattice [61].

TABLE I. Site percolation thresholds and other properties, including r^2, NN, and total z, for the 11 Archimedean lattices with extended neighborhoods, up to the 10th NN. Values of p_c shown to three significant digits are from Ref. [37], while higher precision results (many truncated) are from [a]Ref. [46], [b]Ref. [60], [c]Ref. [51], [d]Ref. [61], [e]exact, [f]by matching, and [g]by bond-to-site transformation.

		Nearest-neighbor number									
Lattice		1	2	3	4	5	6	7	8	9	10
(3^6)	r^2	1	3	4	7	9	12	13	16	19	21
TRI	NN	6	6	6	12	6	6	12	6	12	12
	Total z	6	12	18	30	36	42	54	60	72	84
	p_c	0.500000[e]	0.29026[a]	0.21546[a]	0.13582[a]	0.11574[a]	0.099	0.078	0.071	0.059	0.051
(4^4)	r^2	1	2	4	5	8	9	10	13	16	17
SQ	NN	4	4	4	8	4	4	8	8	4	8
	Total z	4	8	12	20	24	28	36	44	48	56
	p_c	0.592746[b]	0.407254[f]	2891230.[c]	0.196729[c]	0.164712[c]	0.143255[c]	0.115348[c]	0.095766[c]	0.086	0.075
(6^3)	r^2	1	3	4	7	9	12	13	16	19	21
HC	NN	3	6	3	6	6	6	6	3	6	12
	Total z	3	9	12	18	24	30	36	39	45	57
	p_c	0.697040[b]	0.359	0.302960[f]	0.210	0.164	0.135	0.115	0.108	0.092	0.075
(3,6,3,6)	r^2	1	3	4	7	9	12	13	16	19	21
KAG	NN	4	4	6	8	4	6	8	6	8	8
	Total z	4	8	14	22	26	32	40	46	54	62
	p_c	0.652703[e]	0.386	0.263	0.179	0.155	0.126	0.103	0.091	0.079	0.069
(3,4,6,4)	r^2	1	2	3	$2+\sqrt{3}$	4	$4+\sqrt{3}$	$4+2\sqrt{3}$	$5+2\sqrt{3}$	$6+3\sqrt{3}$	$8+2\sqrt{3}$
	NN	4	2	2	4	1	4	7	4	4	4
	Total z	4	6	8	12	13	17	24	28	32	36
	p_c	0.621812[b]	0.524405[b,g]	0.398	0.294	0.279	0.223	0.164	0.145	0.128	0.120
$(3^3, 4^2)$	r^2	1	2	3	$2+\sqrt{3}$	4	5	$4+\sqrt{3}$	7	$4+2\sqrt{3}$	$5+2\sqrt{3}$
	NN	5	2	2	4	2	2	4	2	1	4
	total z	5	7	9	13	15	17	21	23	24	28
	p_c	0.550213[d]	0.449787[f]	0.366	0.279	0.244	0.222	0.186	0.171	0.165	0.144
$(3^2, 4, 3, 4)$	r^2	1	2	3	$2+\sqrt{3}$	$4+\sqrt{3}$	$4+2\sqrt{3}$	$5+2\sqrt{3}$	$7+2\sqrt{3}$	$6+3\sqrt{3}$	$8+2\sqrt{3}$
	NN	5	2	1	8	4	6	6	2	4	2
	Total z	5	7	8	16	20	26	32	34	38	40
	p_c	0.550806[d]	0.449104[f]	0.405	0.237	0.195	0.153	0.129	0.121	0.108	0.096
$(3^4, 6)$	r^2	1	3	4	7	9	12	13	16	19	21
	NN	5	5	5	11	5	5	10	5	10	11
	Total z	5	10	15	26	31	36	46	51	61	72
	p_c	0.579498[b]	0.335	0.249	0.153	0.132	0.114	0.092	0.083	0.069	0.060
$(4, 8^2)$	r^2	1	2	$2+\sqrt{2}$	$3+2\sqrt{2}$	$4+2\sqrt{2}$	$5+2\sqrt{2}$	$6+3\sqrt{2}$	$6+4\sqrt{2}$	$7+4\sqrt{2}$	$9+4\sqrt{2}$
	NN	3	1	4	6	2	2	4	5	4	1
	Total z	3	4	8	14	16	18	22	27	31	32
	p_c	0.729723[b]	0.707107[e,g]	0.399	0.261	0.239	0.213	0.179	0.149	0.132	0.129
$(3, 12^2)$	r^2	1	$2+\sqrt{3}$	$4+2\sqrt{3}$	$5+2\sqrt{3}$	$6+3\sqrt{3}$	$7+4\sqrt{3}$	$8+4\sqrt{3}$	$10+5\sqrt{3}$	$11+6\sqrt{3}$	$12+6\sqrt{3}$
	NN	3	4	4	2	4	8	2	4	6	2
	Total z	3	7	11	13	17	25	27	31	37	39
	p_c	0.807901[e]	0.464	0.312	0.272	0.216	0.159	0.151	0.133	0.112	0.108
(4,6,12)	r^2	1	2	3	$2+\sqrt{3}$	4	$4+\sqrt{3}$	$4+2\sqrt{3}$	$5+2\sqrt{3}$	$6+3\sqrt{3}$	$8+2\sqrt{3}$
	NN	3	1	2	2	1	2	4	2	4	1
	Total z	3	4	6	8	9	11	15	17	21	22
	p_c	0.747801[b,g]	0.724158[g]	0.571	0.421	0.403	0.348	0.251	0.231	0.190	0.180

universality of asymptotic behavior for zp_c for site percolation on all extended-range Archimedean lattices over a wide range of z.

While both plots have a slope near the predicted value from η_c, the points of Fig. 8 fit well the assumption of an intercept equal to zero, while those of Fig. 7 fit to a line with the correct slope but a nonzero intercept, which corresponds to the constant $-b$ in Eq. (13). The data for the various lattices predicts b in the range 2.13 to 3.44, with an average value of ≈3.0. By using Eq. (12) rather than Eq. (13) to fit the

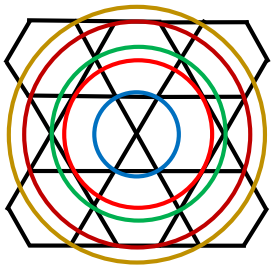

FIG. 6. Illustration showing the first five shells of nearest neighbors (NN) of the kagome (3,6,3,6) lattice. In the first shell (radius $r = 1$), there are 4 NN, in the second shell ($r = \sqrt{3}$), there are 4 NN, in the third shell ($r = 2$), there are 6 NN, in the fourth shell ($r = \sqrt{7}$), there are 8 NN, and in the fifth shell ($r = 3$), there are 4 NN, as listed in Table I. Looking at larger r, we find that the shell index number appears to grow with r as a power law $\sim r^{2.27}$.

thresholds, we get a satisfactory fit of the finite-z behavior without the need of an additional parameter.

We can also look at different lattices that share the same value of $z = z_{\text{total}}$ and compare their thresholds. For example, $z = 12$ corresponds to the TRI-1,2 lattice ($p_c = 0.29026$), the SQ-3 lattice ($p_c = 0.289123$), the HC-1,2,3 lattice ($p_c = 0.302960$), and the (3,4,6,4)-1,2,3,4 lattice ($p_c = 0.294$), where the numbers after the lattice name represents the NN. Notice that the thresholds are close together. Our theoretical formulas give $p_c = 0.37602$ [Eq. (6)], $p_c = 0.30082$ [Eq. (13) with $b = 3$], and $p_c = 0.31341$ [Eq. (11)]. Clearly, Eq. (13) with $b = 3$ gives the best approximation to the actual thresholds.

For a larger $z = 36$, we find the thresholds also close together: TRI-1,2,3,4,5 ($p_c = 0.11574$), SQ-1,...,7 ($p_c = 0.115348$), HC-1,...,7 ($p_c = 0.115$), (3,4,6,4)-1,...,10 ($p_c = 0.120$), and (3^4,6)-1,...,6 ($p_c = 0.114$). The approximation formulas give $p_c = 0.12534$ [Eq. (6)], $p_c = 0.11570$ [Eq. (13) with $b = 3$], and $p_c = 0.11780$ [Eq. (11)]. Once again,

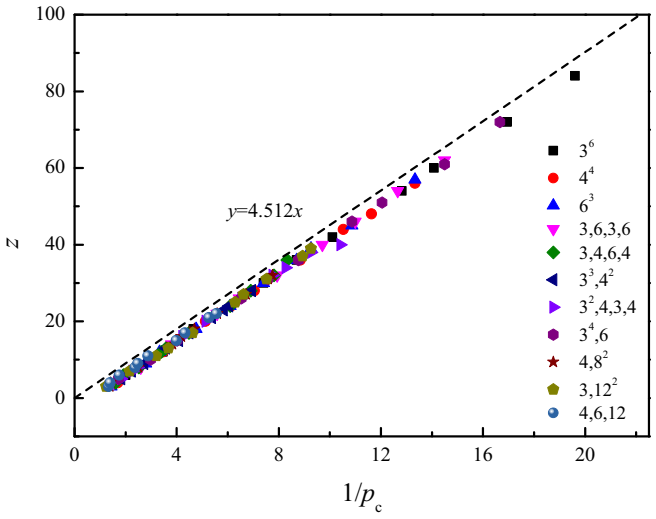

FIG. 7. Plots of z versus $1/p_c$ for the 11 Archimedean lattices with various ranges of NN, using the data of Table I. The virtual straight line is a guideline with a slope of 4.512 and intercept of 0, corresponding to Eq. (6).

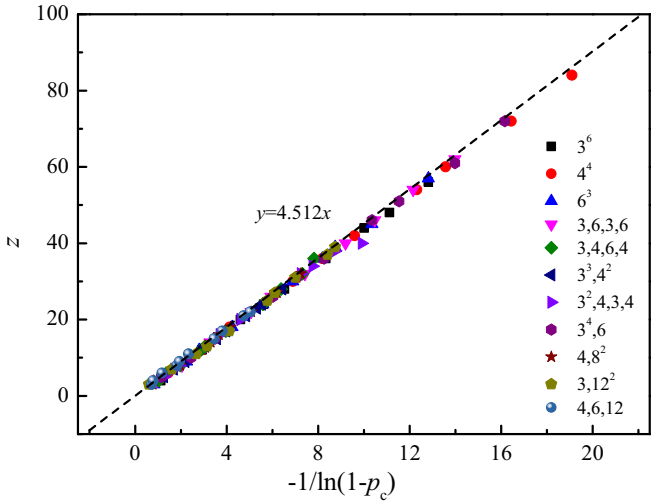

FIG. 8. Plot of z versus $-1/\ln(1 - p_c)$ for the 11 Archimedean lattices with various ranges of NN. The virtual straight line is a guideline with a slope of 4.512 and intercept of 0, corresponding to Eq. (6).

Eq. (13) with $b = 3$ gives the best approximation. To make a better comparison with theory, it would be useful to have the results of the last three lattices above to higher precision.

IV. SITE AND BOND PERCOLATION ON SC, BCC, AND FCC LATTICES WITH EXTENDED CONNECTIONS

Here we carried out extensive Monte Carlo simulations, using a single-cluster growth method [49,50,63]. In this method, many individual clusters are generated from a seeded site on the lattice, and clusters with different sizes s are put in different bins with the range of $(2^n, 2^{n+1} - 1)$ for $n = 0, 1, 2, \ldots$. Clusters still growing when they reach an upper size cutoff (this value is set to avoid wrapping around the boundaries and to limit the run time) are counted in the last bin. Define $n_s(p)$ as the number of clusters (per site) containing s occupied sites as a function of the site or bond occupation probability p. In the scaling limit, in which s is large and $(p - p_c)$ is small such that $(p - p_c)s^\sigma$ is constant, $n_s(p)$ behaves as

$$n_s(p) \sim A_0 s^{-\tau} f[B_0(p - p_c)s^\sigma], \tag{14}$$

where τ, σ, and $f(x)$ are universal (having same values in a given dimension), while A_0 and B_0 are lattice-dependent factors. The probability that a point belongs to a cluster of size greater than or equal to s is given by $P_{\geqslant s} = \sum_{s'=s}^{\infty} s' n_{s'}$, and it follows for large s and small $(p - p_c)s^\sigma$ that $s^{\tau-2}P_{\geqslant s}$ behaves as

$$s^{\tau-2}P_{\geqslant s} \sim A_1 + B_1(p - p_c)s^\sigma + C_1 s^{-\Omega}. \tag{15}$$

Here we also added a correction-to-scaling term with exponent Ω. The A_1, B_1, and C_1 are nonuniversal constants. From the behavior of this quantity, we can easily determine if we are above, near, or below the percolation threshold. One can see Refs. [49,50,63] for more details about the single-cluster method.

With regard to the universal exponents τ, Ω, and σ, in three dimensions, relatively accurate and acceptable results

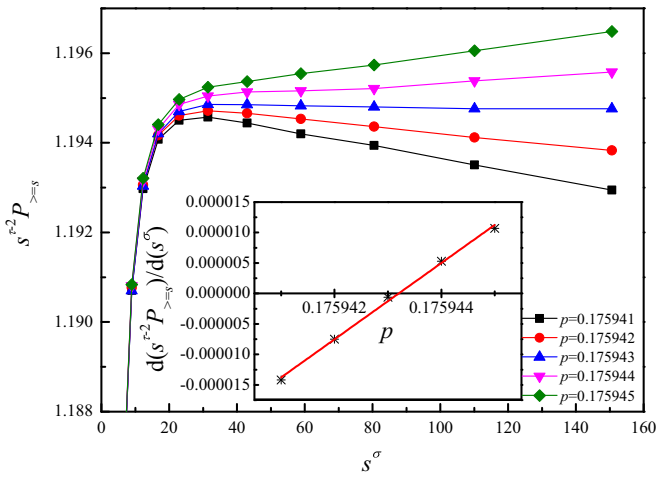

FIG. 9. Plot of $s^{\tau-2}P_{\geqslant s}$ versus s^{σ} with $\tau = 2.18905$ and $\sigma = 0.4522$ for site percolation of the BCC-1,2 lattice under different values of p. The inset indicates the slope of the linear portions of the curves shown in the main figure as a function of p, and the predicted value of $p_c = 0.1759432$ can be calculated from the p intercept.

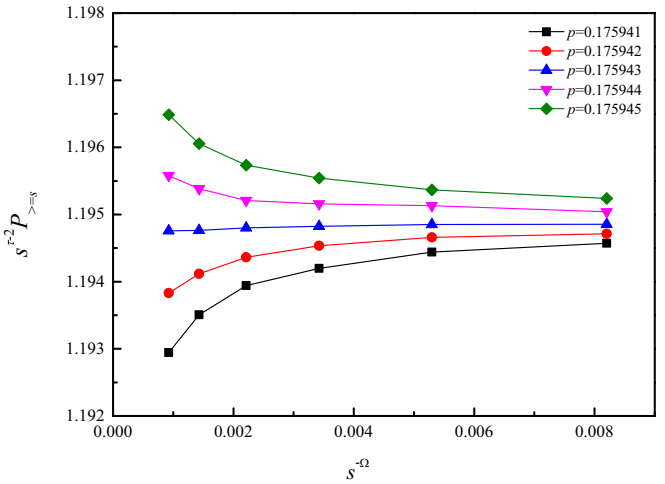

FIG. 10. Plot of $s^{\tau-2}P_{\geqslant s}$ versus $s^{-\Omega}$ with $\tau = 2.18905$ and $\Omega = 0.63$ for site percolation of the BCC-1,2 lattice under different values of p.

are known: 2.18906(8) [64] and 2.18909(5) [65] for τ; 0.64(2) [63], 0.65(2) [66], 0.60(8) [67], and 0.64(5) [68] for Ω; and 0.4522(8) [64], 0.45237(8) [65], and 0.4419 [69] for σ. In our simulations, $\tau = 2.18905(15)$, $\Omega = 0.63(4)$, and $\sigma = 0.4522(2)$ are chosen. Here we take large error bars on these values for the sake of safety.

The upper size cutoff is set to be $s_{\max} = 2^{16}$ occupied sites. Monte Carlo simulations are performed on systems of size $L \times L \times L$ with $L = 512$ under periodic boundary conditions (although the boundaries are actually never reached). Some 10^9 independent samples were produced for BCC and FCC lattices with 2nd and 3rd NN, and 10^8 for the SC lattice with nth NN, with n from 5 to 13. The number of clusters greater than or equal to size s could be found based on the data from our simulations, and the quantity $s^{\tau-2}P_{\geqslant s}$ could easily be calculated.

A. Site percolation

We use the notation BCC-$a, b, \ldots$ to indicate a BCC lattice with the ath NN, the bth NN, etc., and similarly for the FCC and SC lattices.

Figure 9 shows the relation of $s^{\tau-2}P_{\geqslant s}$ versus s^{σ} for site percolation of the BCC-1,2 lattice, under probabilities $p = 0.175941$, 0.175942, 0.175943, 0.175944, and 0.175945. (Preliminary work narrowed the search to this range.) For small clusters, we can see a steep rise of $s^{\tau-2}P_{\geqslant s}$ corresponding to the finite-size-effect term, $s^{-\Omega}$, while for large clusters, the plot shows linear behavior as expected from Eq. (15). The linear portion of the curve become more nearly horizontal when p is close to p_c. The estimated value of p_c can then be deduced using $d(s^{\tau-2}P_{\geqslant s})/d(s^{\sigma}) \sim B_1(p - p_c)$, as shown in the inset of Fig. 9, where $p_c = 0.1759432$ can be estimated from the p intercept of the plot of the derivative versus p.

When p is close to p_c, a plot of $s^{\tau-2}P_{\geqslant s}$ versus $s^{-\Omega}$ is useful to estimate the percolation threshold. Figure 10 shows this plot for the BCC-1,2 lattice under probabilities $p = 0.175941$, 0.175942, 0.175943, 0.175944, and 0.175945. Linear behavior for large s (small abscissa) can be seen when p is very close to p_c, while when p is away from p_c, the curves show obvious deviations from linearity for large s. Based on these curves, the range $0.175943 < p_c < 0.175944$ can be concluded, which is consistent with the value we deduced from Fig. 9, $p_c = 0.1759432$.

Thus, we conclude that the site percolation threshold of the BCC-1,2 lattice to be $p_c = 0.1759432(8)$, where the number in parentheses represents the estimated error in the last digit, by comprehensively considering the two methods mentioned above, as well as the errors for the values of τ, Ω, and σ. The simulation results for the other three lattices we considered (BCC-1,2,3, FCC-1,2, and FCC-1,2,3) are shown in the Supplemental Material [62,70] in Figs. S1–S6, and the corresponding

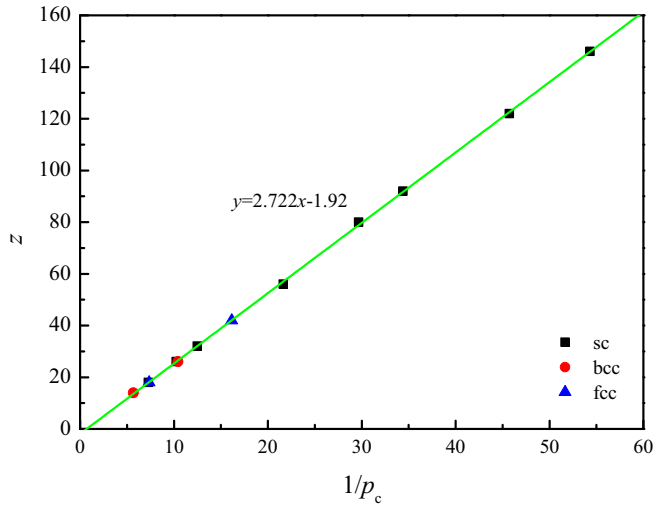

FIG. 11. Plot of z versus $1/p_c$ for the three-dimensional lattices shown in Table II. The green line is a fit through the data and has a slope 2.722(11), close to the predicted value 2.7351 from Eq. (7), and intercept $-b = -1.92(28)$.

TABLE II. Site percolation thresholds for the SC, BCC, and FCC lattices with various ranges of NN. The BCC and FCC results were determined here, while the results for the SC lattice come from Ref. [51]. Previous results are also shown.

Lattice	z	p_c	zp_c	Previous values
BCC-1,2	14	0.1759432(8)	2.4632	0.175 [29], 0.1686(20) [33]
SC-1,2	18	0.1373045(5)	2.4715	0.137 [29], 0.136 [34]
				0.1372(1) [42]
FCC-1,2	18	0.1361408(8)	2.4505	0.136 [29]
SC-1,2,3	26	0.0976444(6)	2.5388	0.097 [29], 0.0976(1) [42]
BCC-1,2,3	26	0.0959084(6)	2.4936	0.095 [30]
SC-1,2,3,4	32	0.0801171(9)	2.5637	0.10000(12) [43]
FCC-1,2,3	42	0.0618842(8)	2.5991	0.061 [30], 0.0610(5) [34]
SC-1,. . .,5	56	0.0461815(5)	2.5861	
SC-1,. . .,6	80	0.0337049(9)	2.6964	
SC-1,. . .,7	92	0.0290800(10)	2.6754	
SC-1,. . .,8	122	0.0218686(6)	2.6680	
SC-1,. . .,9	146	0.0184060(10)	2.6873	

thresholds are summarized in Table II. Previously reported results are also shown, and it can be seen that the accuracy of the thresholds has been greatly increased. Our results are generally consistent with previous works, except for the case of the SC-1,2,3,4 lattice where a previous result from Ref. [43] was evidently in error [49].

For the convenience of the following analysis, in Table II, we also show our former site percolation thresholds for SC-$1,\ldots,n$ ($2 \leqslant n \leqslant 9$) lattices [51]. In addition, the values of zp_c are also shown in the fourth column of Table II. With the increase of coordination number z, the value of zp_c shows a gradual increase. Further investigations are performed by plotting the relation of z versus $1/p_c$ and z versus $-1/\ln(1-p_c)$, as shown in Figs. 11 and 12, respectively. One can see that the results of different lattices collapse onto a line, which has a slope of 2.722 for Fig. 11 and 2.721 for Fig. 12, both very near to our predicted universal asymptotic value of $zp_c = 2.7351$ of Eq. (7).

B. Bond percolation

For bond percolation on BCC-1,2 lattice, under probabilities $p = 0.101211$, 0.101212, 0.101213, 0.101214, and 0.101215, the corresponding plots are shown in Figs. 13 and 14. Similarly to the procedure for site percolation, the bond percolation threshold $p_c = 0.1012133(7)$ is estimated for this system. It turns out that this system is identical to the SC-3,4 lattice, and in Ref. [49] we found the identical value of the threshold for that lattice. The simulation results for the other 12 bond lattices that we considered [including BCC-1,2,3, FCC-1,2, FCC-1,2,3, and SC-$1,\ldots,n$ ($5 \leqslant n \leqslant 13$)] are shown in the Supplemental Material [62,70] in Figs. S7–S30, and the corresponding bond percolation thresholds are summarized in Table III.

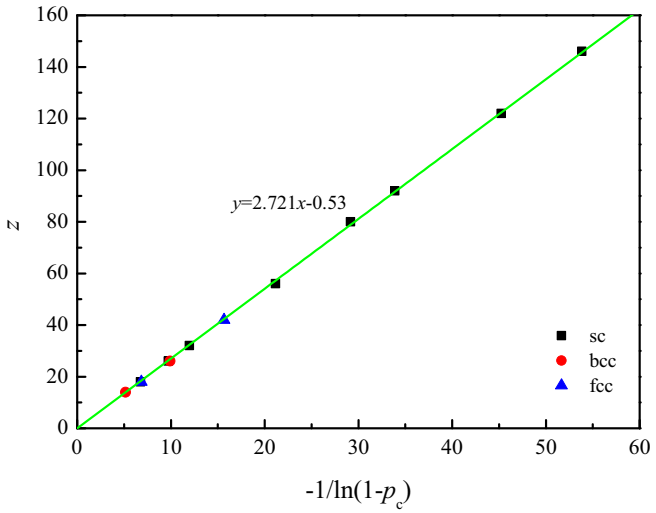

FIG. 12. Plot of z versus $-1/\ln(1-p_c)$ for site percolation threshold for the three-dimensional lattices listed in Table II. The green line is a linear fit through the data and has a slope 2.721(11), close to the predicted value 2.7351 from Eq. (7), and intercept $-0.53(27)$.

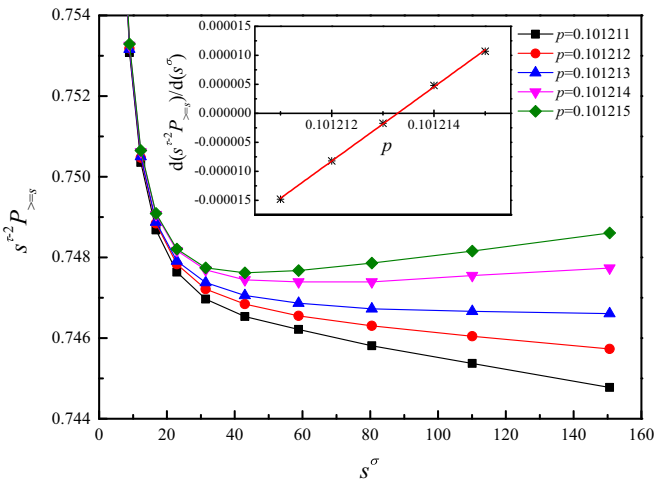

FIG. 13. Plot of $s^{\tau-2}P_{\geqslant s}$ vs. s^{σ} with $\tau = 2.18905$ and $\sigma = 0.4522$ for bond percolation of the BCC-1,2 lattice under different values of p. The inset indicates the slope of the linear portions of the curves shown in the main figure as a function of p, and the estimated value of $p_c = 0.1012133$ can be deduced from the p intercept.

TABLE III. Bond percolation thresholds for the SC, BCC, and FCC lattices with various ranges of NN. The values for SC-1,2, SC-1,2,3, and SC-1,2,3,4 lattices come from Ref. [50], while the results for other lattices were determined here. The identical threshold value for BCC-1,2 was previously found by us for the equivalent SC-2,3 lattice [49]. The only other previous value appears to be 0.0991(5) for BCC-1,2 of Ref. [33].

Lattice	z	p_c	zp_c
BCC-1,2	14	0.1012133(7)	1.4170
SC-1,2	18	0.0752326(6)	1.3542
FCC-1,2	18	0.0751589(9)	1.3529
SC-1,2,3	26	0.0497080(10)	1.2924
BCC-1,2,3	26	0.0492760(10)	1.2812
SC-1,2,3,4	32	0.0392312(8)	1.2554
FCC-1,2,3	42	0.0290193(7)	1.2188
SC-1,. . .,5	56	0.0210977(7)	1.1815
SC-1,. . .,6	80	0.0143950(10)	1.1516
SC-1,. . .,7	92	0.0123632(8)	1.1374
SC-1,. . .,8	122	0.0091337(7)	1.1143
SC-1,. . .,9	146	0.0075532(8)	1.1028
SC-1,. . .,10	170	0.0064352(8)	1.0940
SC-1,. . .,11	178	0.0061312(8)	1.0914
SC-1,. . .,12	202	0.0053670(10)	1.0841
SC-1,. . .,13	250	0.0042962(8)	1.0741

In Table III, we also list some previously known values, for lattices with various ranges of NN. We show the value of zp_c in the fourth column of that table. The results show that the value of zp_c decreases from 1.4170 to 1.0741 with the increase of coordination number z from 14 to 250. In Fig. 15, we plot zp_c versus z^{-x}, and find that a good linear fit is obtained when $x \approx 2/3$. This is in agreement with the theoretical predictions of Refs. [9] and [53]. Figure 15 also exhibits an intercept very close to 1, implying that the Bethe result $p_c = 1/(z-1)$ accurately holds as $z \to \infty$.

V. CONCLUSIONS

To summarize, in this paper, correlations between percolation threshold p_c and coordination number z for lattice models with compact neighborhoods, including both the asymptotic and finite-z behavior, are investigated systematically. To study these correlations, extensive Monte Carlo simulations are carried out for site and bond percolation on BCC, FCC lattices with 2nd and 3rd NN and bond percolation on SC lattice with up to 13th NN. We find precise estimates of the percolation thresholds for these systems. We also include previous results by ourselves and others to make our analysis.

For site percolation, two-dimensional Archimedean lattices and three-dimensional SC, BCC, and FCC lattices with compact neighborhoods (up to 10th NN for Archimedean lattices, 3rd for BCC and FCC lattices, and 9th for SC lattice) are analyzed by plotting z versus $1/p_c$ and z versus $-1/\ln(1-p_c)$. We find, in a given dimension, nearly all the plots overlap in a line,

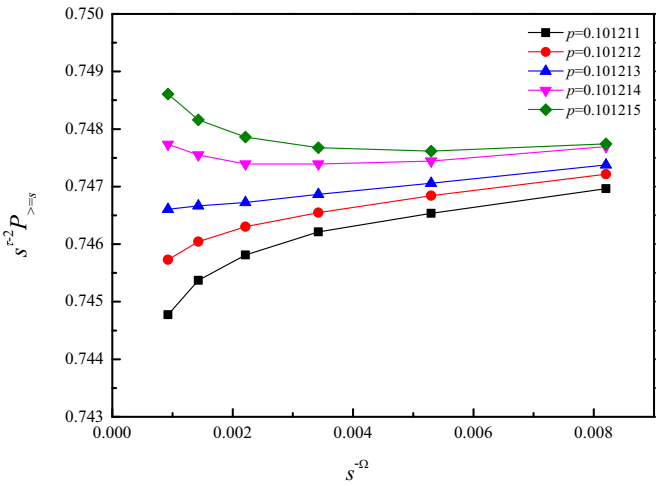

FIG. 14. Plot of $s^{\tau-2}P_{\geqslant s}$ versus $s^{-\Omega}$ with $\tau = 2.18905$ and $\Omega = 0.63$ for bond percolation of the BCC-1,2 lattice under different values of p.

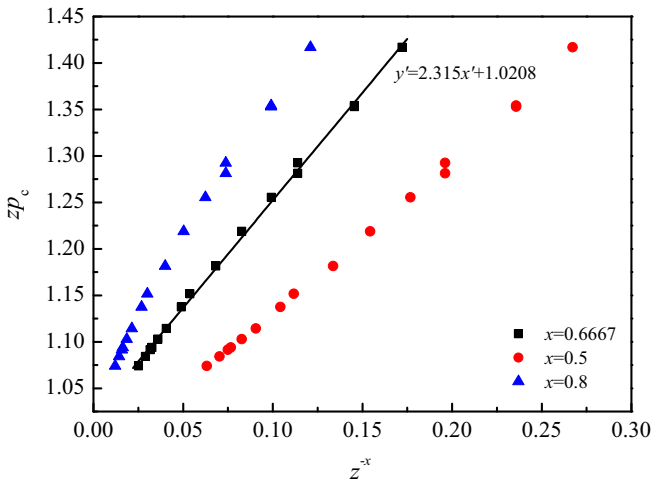

FIG. 15. Plot of zp_c versus z^{-x} with $x = 0.5$, 0.6667, and 0.8 for the bond percolation thresholds of all three-dimensional lattices listed in Table III, showing that Eq. (2) with $x = 2/3$ gives a good representation of the behavior of zp_c. The intercept of the line for the fit with $x = 2/3$, 1.0208(22) is close to 1 as is required from Eq. (2). The slope gives $a_1 = 2.315(24)$.

with the slopes consistent with our predicted values of $zp_c \sim 4\eta_c = 4.51235$ in two dimensions and $zp_c \sim 8\eta_c = 2.7351$ in three dimensions. The plot of z versus $-1/\ln(1-p_c)$ gives a good fit of the behavior including the finite-z corrections, with no additional adjustable parameters.

For bond percolation in three dimensions, the thresholds of SC, BCC, and FCC lattices with compact neighborhoods (up to 3rd for BCC and FCC lattices and 13th for SC lattice) confirm the finite-z corrections of Eq. (2) with $x = 2/3$ predicted by Frei and Perkins [53] and Xu *et al.* [9] and verify that Bethe-lattice behavior $p_c \sim 1/(z-1)$ holds for large z.

The work in this paper indicates that the asymptotic behavior of zp_c for compact neighborhoods, at least in two and three dimensions, is universal, depending only on the dimension of the system but not on the type of lattice. Of course, this universality is not as strong as the universality of critical exponents and scaling functions, which applies to all systems of a given dimensionality. Here the behavior depends on whether the percolation type is site or bond. For bond percolation, the universality in the formula for p_c is rather robust since for large z, a critical system acts like a Bethe lattice. For site percolation, the universality we discuss here refers to all systems of compact neighbors that fall in a circular or spherical region. If the range of the neighborhood is in a different shape, such as an elongated one, then one would use Eq. (6) with η_c being the continuum threshold for objects of that shape. Note that for both site and bond percolation, $p_c \sim c/z$ for large z, but the coefficient c differs for the two types of percolation. It would be interesting of course to further investigate these ideas for neighborhoods of different shapes and in higher dimensions. (Systems of other shapes have been investigated in Refs. [32], [26], and [45], for example.)

Overall, we see that percolation with extended-range bonds is interesting for both site and bond percolation, has many connections with literature in the field, and shows a form of universality. The formulas of Eq. (1) (for site percolation) and Eq. (2) (for bond percolation) can be used to get good estimates for the thresholds for extended-range percolation models, as we have verified here for many systems.

ACKNOWLEDGMENTS

The authors are grateful to the Advanced Analysis and Computation Center of CUMT for the award of CPU hours to accomplish this work. This work is supported by "Fundamental Research Funds for the Central Universities" under Grant No. 2020ZDPYMS31.

[1] S. R. Broadbent and J. M. Hammersley, Percolation processes: I. Crystals and mazes, Math. Proc. Cambr. Philos. Soc. **53**, 629 (1957).

[2] D. Stauffer and A. Aharony, *Introduction to Percolation Theory, 2nd ed.* (CRC Press, Boca Raton, FL, 1994).

[3] S. F. Bolandtaba and A. Skauge, Network modeling of EOR processes: A combined invasion percolation and dynamic model for mobilization of trapped oil, Transp. Porous Media **89**, 357 (2011).

[4] V. V. Mourzenko, J.-F. Thovert, and P. M. Adler, Permeability of isotropic and anisotropic fracture networks, from the percolation threshold to very large densities, Phys. Rev. E **84**, 036307 (2011).

[5] C. L. Henley, Statics of a "Self-Organized" Percolation Model, Phys. Rev. Lett. **71**, 2741 (1993).

[6] N. Guisoni, E. S. Loscar, and E. V. Albano, Phase diagram and critical behavior of a forest-fire model in a gradient of immunity, Phys. Rev. E **83**, 011125 (2011).

[7] C. Moore and M. E. J. Newman, Epidemics and percolation in small-world networks, Phys. Rev. E **61**, 5678 (2000).

[8] R. M. Ziff, Percolation and the pandemic, Physica A **568**, 125723 (2021).

[9] W. Xu, J. Wang, H. Hu, and Y. Deng, Critical polynomials in the nonplanar and continuum percolation models, Phys. Rev. E **103**, 022127 (2021).

[10] S. Mertens and C. Moore, Continuum percolation thresholds in two dimensions, Phys. Rev. E **86**, 061109 (2012).

[11] J. A. Quintanilla and R. M. Ziff, Asymmetry in the percolation thresholds of fully penetrable disks with two different radii, Phys. Rev. E **76**, 051115 (2007).

[12] Y. Yu. Tarasevich and A. V. Eserkepov, Percolation thresholds for discorectangles: Numerical estimation for a range of aspect ratios, Phys. Rev. E **101**, 022108 (2020).

[13] Y. Kantor, Three-dimensional percolation with removed lines of sites, Phys. Rev. B **33**, 3522 (1986).

[14] J. Zierenberg, N. Fricke, M. Marenz, F. P. Spitzner, V. Blavatska, and W. Janke, Percolation thresholds and fractal dimensions for square and cubic lattices with long-range correlated defects, Phys. Rev. E **96**, 062125 (2017).

[15] K. J. Schrenk, M. R. Hilário, V. Sidoravicius, N. A. M. Araújo, H. J. Herrmann, M. Thielmann, and A. Teixeira, Critical Fragmentation Properties of Random Drilling: How Many Holes Need to be Drilled to Collapse a Wooden Cube? Phys. Rev. Lett. **116**, 055701 (2016).

[16] P. Grassberger, Universality and asymptotic scaling in drilling percolation, Phys. Rev. E **95**, 010103(R) (2017).

[17] J.-O. Choi and U. Yu, Bootstrap and diffusion percolation transitions in three-dimensional lattices, J. Stat. Mech.: Theory Exp. (2020) 063218.

[18] J.-O. Choi and U. Yu, Newman-ziff algorithm for the bootstrap percolation: Application to the archimedean lattices, J. Comput. Phys. **386**, 1 (2019).

[19] M. A. Di Muro, S. V. Buldyrev, and L. A. Braunstein, Reversible bootstrap percolation: Fake news and fact checking, Phys. Rev. E **101**, 042307 (2020).

[20] M. A. Di Muro, L. D. Valdez, H. Eugene Stanley, S. V. Buldyrev, and L. A. Braunstein, Insights into bootstrap percolation: Its equivalence with k-core percolation and the giant component, Phys. Rev. E **99**, 022311 (2019).

[21] J. Wang, Z. Zhou, Q. Liu, T. M. Garoni, and Y. Deng, High-precision Monte Carlo study of directed percolation in (d + 1) dimensions, Phys. Rev. E **88**, 042102 (2013).

[22] P. Grassberger, Logarithmic corrections in (4 + 1)-dimensional directed percolation, Phys. Rev. E **79**, 052104 (2009).

[23] P. Grassberger, Local persistence in directed percolation, J. Stat. Mech.: Theory Exp. (2009) P08021.

[24] I. Jensen, Low-density series expansions for directed percolation: III. Some two-dimensional lattices, J. Phys. A: Math. Gen. **37**, 6899 (2004).

[25] Z. Koza, G. Kondrat, and K. Suszczyński, Percolation of overlapping squares or cubes on a lattice, J. Stat. Mech.: Theory Exp. (2014) P11005.

[26] Z. Koza and J. Poła, From discrete to continuous percolation in dimensions 3 to 7, J. Stat. Mech.: Theory Exp. (2016) 103206.

[27] J. M. Kleinberg, Navigation in a small world, Nature **406**, 845 (2000).

[28] L. M. Sander, C. P. Warren, and I. M. Sokolov, Epidemics, disorder, and percolation, Physica A **325**, 1 (2003).

[29] N. W. Dalton, C. Domb, and M. F. Sykes, Dependence of critical concentration of a dilute ferromagnet on the range of interaction, Proc. Phys. Soc. **83**, 496 (1964).

[30] C. Domb and N. W. Dalton, Crystal statistics with long-range forces: I. The equivalent neighbour model, Proc. Phys. Soc. **89**, 859 (1966).

[31] C. Domb, A note on the series expansion method for clustering problems, Biometrika **59**, 209 (1972).

[32] M. Gouker and F. Family, Evidence for classical critical behavior in long-range site percolation, Phys. Rev. B **28**, 1449 (1983).

[33] G. R. Jerauld, L. E. Scriven, and H. T. Davis, Percolation and conduction on the 3d Voronoi and regular networks: A second case study in topological disorder, J. Phys. C: Solid State **17**, 3429 (1984).

[34] T. R. Gawron and Marek Cieplak, Site percolation thresholds of fcc lattice, Acta Phys. Pol. A **80**, 461 (1991).

[35] C. d'Iribarne, G. Rasigni, and M. Rasigni, Determination of site percolation transitions for 2d mosaics by means of the minimal spanning tree approach, Phys. Lett. A **209**, 95 (1995).

[36] C. d'Iribarne, M. Rasigni, and G. Rasigni, Minimal spanning tree and percolation on mosaics: Graph theory and percolation, J. Phys. A: Math. Gen. **32**, 2611 (1999).

[37] C. d'Iribarne, M. Rasigni, and G. Rasigni, From lattice long-range percolation to the continuum one, Phys. Lett. A **263**, 65 (1999).

[38] S. Reimann and A. Tupak, Can constrained percolation be approximated by Bernoulli percolation? J. Phys. A: Math. Gen. **35**, 10219 (2002).

[39] K. Malarz and S. Galam, Square-lattice site percolation at increasing ranges of neighbor bonds, Phys. Rev. E **71**, 016125 (2005).

[40] S. Galam and K. Malarz, Restoring site percolation on damaged square lattices, Phys. Rev. E **72**, 027103 (2005).

[41] M. Majewski and K. Malarz, Square lattice site percolation thresholds for complex neighbourhoods, Acta Phys. Pol. B **38**, 2191 (2007).

[42] Ł. Kurzawski and K. Malarz, Simple cubic random-site percolation thresholds for complex neighbourhoods, Rep. Math. Phys. **70**, 163 (2012).

[43] K. Malarz, Simple cubic random-site percolation thresholds for neighborhoods containing fourth-nearest neighbors, Phys. Rev. E **91**, 043301 (2015).

[44] M. Kotwica, P. Gronek, and K. Malarz, Efficient space virtualization for the Hoshen-Kopelman algorithm, Int. J. Mod. Phys. C **30**, 1950055 (2019).

[45] K. Malarz, Site percolation thresholds on triangular lattice with complex neighborhoods, Chaos **30**, 123123 (2020).

[46] K. Malarz, Percolation thresholds on a triangular lattice for neighborhoods containing sites up to the fifth coordination zone, Phys. Rev. E **103**, 052107 (2021).

[47] Y. Ouyang, Y. Deng, and H. W. J. Blöte, Equivalent-neighbor percolation models in two dimensions: Crossover between mean-field and short-range behavior, Phys. Rev. E **98**, 062101 (2018).

[48] Y. Deng, Y. Ouyang, and H. W. J. Blöte, Medium-range percolation in two dimensions, J. Phys.: Conf. Ser. **1163**, 012001 (2019).

[49] Z. Xun and R. M. Ziff, Precise bond percolation thresholds on several four-dimensional lattices, Phys. Rev. Research **2**, 013067 (2020).

[50] Z. Xun and R. M. Ziff, Bond percolation on simple cubic lattices with extended neighborhoods, Phys. Rev. E **102**, 012102 (2020).

[51] Z. Xun, D. Hao, and R. M. Ziff, Site percolation on square and simple cubic lattices with extended neighborhoods and their continuum limit, Phys. Rev. E **103**, 022126 (2021).

[52] M. D. Penrose, On the spread-out limit for bond and continuum percolation, Ann. Appl. Probab. **3**, 253 (1993).

[53] S. Frei and E. Perkins, A lower bound for p_c in range-r bond percolation in two and three dimensions, Electron. J. Probab. **21**, 56 (2016).

[54] J. Hong, An upper bound for p_c in range-r bond percolation in two and three dimensions arXiv:2107.14173.

[55] Z. Koza, Critical $p = 1/2$ in percolation on semi-infinite strips, Phys. Rev. E **100**, 042115 (2019).

[56] J. Li and M. Ostling, Precise percolation thresholds of two-dimensional random systems comprising overlapping ellipses, Physica A **462**, 940 (2016).

[57] C. D. Lorenz and R. M. Ziff, Precise determination of the critical percolation threshold for the three-dimensional "Swiss cheese" model using a growth algorithm, J. Chem. Phys. **114**, 3659 (2001).

[58] S. Torquato and Y. Jiao, Effect of dimensionality on the continuum percolation of overlapping hyperspheres and hypercubes. II. Simulation results and analyses, J. Chem. Phys. **137**, 074106 (2012).

[59] G. Gori and A. Trombettoni, Conformal invariance in three dimensional percolation, J. Stat. Mech.: Theory Exp. (2015) P07014.

[60] J. L. Jacobsen, High-precision percolation thresholds and Potts-model critical manifolds from graph polynomials, J. Phys. A: Math. Theor. **47**, 135001 (2014).

[61] P. N. Suding and R. M. Ziff, Site percolation thresholds for Archimedean lattices, Phys. Rev. E **60**, 275 (1999).

[62] See Supplemental Material at http://link.aps.org/supplemental/10.1103/PhysRevE.105.024105 for slopes and intercepts of plots in Fig. 8.

[63] C. D. Lorenz and R. M. Ziff, Precise determination of the bond percolation thresholds and finite-size scaling corrections for the sc, fcc, and bcc lattices, Phys. Rev. E **57**, 230 (1998).

[64] H. G. Ballesteros, L. A. Fernández, V. Martín-Mayor, A. Muñoz Sudupe, G. Parisi, and J. J. Ruiz-Lorenzo, Measures of critical exponents in the four-dimensional site percolation, Phys. Lett. B **400**, 346 (1997).

[65] X. Xu, J. Wang, J.-P. Lv, and Y. Deng, Simultaneous analysis of three-dimensional percolation models, Front. Phys. **9**, 113 (2014).

[66] J.-C. Gimel, T. Nicolai, and D. Durand, Size distribution of percolating clusters on cubic lattices, J. Phys. A: Math. Gen. **33**, 7687 (2000).

[67] D. Tiggemann, Simulation of percolation on massively-parallel computers, Int. J. Mod. Phys. C **12**, 871 (2001).

[68] H. G. Ballesteros, L. A. Fernández, V. Martín-Mayor, A. Muñoz Sudupe, G. Parisi, and J. J. Ruiz-Lorenzo, Scaling corrections: Site percolation and Ising model in three dimensions, J. Phys. A: Math. Gen. **32**, 1 (1999).

[69] J. A. Gracey, Four loop renormalization of theory in six dimensions, Phys. Rev. D **92**, 025012 (2015).

[70] See Supplemental Material at http://link.aps.org/supplemental/10.1103/PhysRevE.105.024105 for the simulation results.